JBC Papers in Press. Published on April 12, 2011 as Manuscript M110.210294
The latest version is at http://www.jbc.org/cgi/doi/10.1074/jbc.M110.210294

Cyclic AMP activates TRPC6 channels via PI3K-PKB-MEK-ERK1/2 signaling pathway

Bing Shen[1,2,3], Hiu-Yee Kwan[1,2], Xin Ma[1,2], Ching-On Wong[1,2],
Juan Du[1,2,3], Yu Huang[1,2], Xiaoqiang Yao[1,2,*]

From [1]Li Ka Shing Institute of Health Sciences and [2]School of Biomedical Sciences, Faculty of Medicine, Chinese University of Hong Kong, Hong Kong, China, [3]Department of Physiology, An Hui Medical University, He Fei, China.

Running title: Cyclic AMP activates TRPC6

*, Address correspondence to Xiaoqiang Yao, Ph.D
School of Biomedical Sciences, Faculty of Medicine
The Chinese University of Hong Kong
Hong Kong
China
Fax: 852-26035022
Email: yao2068@cuhk.edu.hk

ABSTRACT

Cyclic AMP (cAMP) is an important second messenger that executes diverse physiological function in living cells. In the present study, we investigated the effect of cAMP on canonical transient receptor potential 6 channels (TRPC6) in TRPC6-expressing HEK293 cells and glomerular mesangial cells. The results showed that 500 μM 8-Br-cAMP, a cell permeable analog of cAMP, elicited intracellular Ca^{2+} ($[Ca^{2+}]_i$) rises and stimulated a cation current at whole-cell level in TRPC6-expressing HEK293 cells. The effect of cAMP diminished in the presence of phosphatidylinositol 3-kinase (PI3K) inhibitors wortmannin and LY294002, or mitogen-activated protein kinase kinase (MEK) inhibitors PD98059, U0126 and MEK inhibitor I. 8-Br-cAMP also induced phosphorylation of MEK and extracellular signals regulated kinase 1 and 2 (ERK1/2). Conversion of serine to glycine at an ERK1/2 phosphorylation site (S281G) abolished the cAMP activation on TRPC6, as determined by whole-cell and cell-attached single-channel patch recordings. Experiments based on a panel of pharmacological inhibitors or activators suggested that the cAMP action on TRPC6 was not mediated by protein kinase A (PKA), protein kinase G (PKG) or exchange protein activated by cAMP (EPAC). Total internal fluorescence reflection microscopy (TIRFM) showed that 8-Br-cAMP did not alter the trafficking of TRPC6 to the plasma membrane. We also found that, in glomerular mesangial cells, glucagon-induced $[Ca^{2+}]_i$ rises are mediated through cAMP-PI3K-PKB-MEK-ERK1/2-TRPC6 signaling pathway. In summary, this study uncovered a novel TRPC6 activation mechanism, in which cAMP activates TRPC6 via PI3K-PKB-MEK-ERK1/2 signaling pathway.

INTRODUCTION

Canonical transient receptor potential 6 channels (TRPC6) are Ca^{2+}-permeable non-selective cation channels. The channels are ubiquitously expressed and play diverse functional roles including vascular smooth muscle contraction, cell proliferation, and kidney glomerular filtration (1-3). Mutation in TRPC6 causes familial focal segmental glomerulosclerosis, which is characterized by proteinuria and progressive decline in renal function (4,5). TRPC6 is activated by diverse cellular signals, including agonists at G_q protein-coupled receptors and diacylglycerol (DAG) (6). Protein phosphorylation has complex regulation on the channels. CaMKII and a Src family receptor tyrosine kinase Fyn activate TRPC6 (7,8), while protein kinase C (PKC) and PKG inactivate the channel (1,9,10). PKA can also phosphorylate TRPC6, although the phosphorylation does not appear to affect cation permeation (11). In general, the mechanisms of TRPC6 activation and regulation are still not well understood.

Cyclic AMP is an important second messenger (12). Numerous physiological factors including hormone, cytokine, autocrine and paracrine agents, can activate membrane-bound adenylyl cyclases, resulting in cytosolic cAMP elevation. The elevated cAMP then acts on multiple downstream targets to regulate cellular responses (13). Some well-known downstream targets of cAMP include PKA (14), cyclic nucleotide-gated (CNG) channels, (14) EPAC (14), and PKG (15,16). Accumulating amount of evidences show that cAMP can also initiate another signaling cascade by activating PI3K-protein kinase B (PKB), which subsequently stimulates MEK and ERK1/2 (17-20). Interestingly, this signaling cascade of cAMP-PI3K-PKB-MEK-ERK1/2 appears to play a key role in glucagon-induced

proliferation of renal mesangial cells (21,22). Glucagon is a major hormone that can bind to specific Gs protein-coupled receptors to activate glycogenolytic and gluconeogenic pathways, causing blood glucose levels to increase. An elevated fasting glucagon levels (hyperglucagonemia) may contribute to the development of diabetes (23). High glucagon may also stimulate the growth and proliferation of glomerular mesangial cells, resulting in subsequent mesangial expansion, glomerulosclerosis, and glomerular injury (22,24). Recently, Li et al. reported that glucagon-induced proliferation of mesangial cells is mediated by a signaling cascade involving cAMP, ERK1/2 and $[Ca^{2+}]_i$ rises (21,22). However, it is not clear whether the $[Ca^{2+}]_i$ rises are related to extracellular Ca^{2+} influx, and if yes, which Ca^{2+}-permeable channels mediate the Ca^{2+} influx.

In the present study, we investigated the effect of cAMP on TRPC6-mediated Ca^{2+} influx and cation current in TRPC6-expressing human embryonic kidney (HEK) 293 cells. Our results demonstrated for the first time that cAMP activates TRPC6-mediated Ca^{2+} influx and cation current, and that the action is mediated through PI3K-PKB-MEK-ERK1/2 signaling pathway. Furthermore, we showed that this mechanism plays a key role in glucagon-induced $[Ca^{2+}]_i$ rise in renal glomerular mesangial cells.

EXPERIMENTAL PROCEDURES

Cell culture, cDNA Expression and siRNA delivery

HEK 293 cells were obtained from the American Type Culture Collection. All cDNA constructs were transiently transfected into HEK293 cells using Lipofectamine 2000. The cells were used for experiments 48-72 h post-transfection. The cells were cultured in DMEM supplemented with 10% FBS and 100 IU/ml penicillin G and 0.1 mg/ml streptomycin. Cells were grown at 37°C in a 5% CO_2 humidified incubator.

Glomerular mesangial cells were isolated from male Sprague-Dawley rats (260-280 g) using the graded sieving technique based on the protocol described elsewhere (25,26). Briefly, isolated glomeruli were digested by collagenase (2 mg/ml) for 45 min at 37°C. After several washes, cells were grown in RPMI 1640 supplemented with 17% FBS, 100 IU/ml penicillin G and 0.1 mg/ml streptomycin at 37°C in a 5% CO_2 humidified incubator. In this study, glomerular mesangial cells from the passage three to the passage five were used. For siRNA studies, TRPC6-specific siRNA or its scrambled control were transfected into glomerular mesangial cells using electroporation with Nucleofector II following the procedure in manufacturer's instruction manual. The cells were used for Ca^{2+} measurement and immunoblots experiments 40 hrs after electroporation. The nucleotide sequence of TRPC6-specific siRNA was GCAGCAUCAUUCAUUGCAAGAUUUA (27).

An expanded Materials and Methods section is available at http://www.jbc.org in the online Supplemental Data.

RESULTS

Cyclic AMP induces $[Ca^{2+}]_i$ oscillations in TRPC6-expressing HEK293 cells

Mouse TRPC6 was transiently expressed in HEK293 cells. 8-Br-cAMP (500 μM), a cell-permeable analog of cAMP, elicited oscillatory $[Ca^{2+}]_i$ rises in TRPC6-expressing cells but not in wild-type HEK293 cells or in vector-transfected cells (Fig. 1A, C and D). Although 8-Br-cAMP is membrane permeable, its membrane permeability is poor (15), therefore a relatively high concentration of 500 μM was employed. If TRPC6-expressing cells were placed in a Ca^{2+}-free bath solution ($0Ca^{2+}$-PSS), 8-Br-cAMP failed to elicit such

$[Ca^{2+}]_i$ rises (Fig. 1C and D), suggesting an obligated requirement for Ca^{2+} entry in the $[Ca^{2+}]_i$ oscillations. Because $[Ca^{2+}]_i$ oscillations are also known to be related to Ca^{2+} release from intracellular Ca^{2+} stores (28,29), the role of intracellular Ca^{2+} release was explored. It was found that, after depletion of intracellular Ca^{2+} stores using thapsigargin (TG, 4 μM) for 10 min, 8-Br-cAMP (500 μM) was only able to induce a single $[Ca^{2+}]_i$ transient without further $[Ca^{2+}]_i$ oscillations (Fig. 1B). However, thapsigargin treatment had no effect on the percentage of cells that could respond to cAMP and the peak magnitude of the first $[Ca^{2+}]_i$ transient (Fig. 1B, C and D). These data suggest that, while the first $[Ca^{2+}]_i$ transient is due to Ca^{2+} influx but not intracellular store Ca^{2+} release, the subsequent $[Ca^{2+}]_i$ oscillations may be related to store Ca^{2+} release. Because we are interested in TRPC6-mediated Ca^{2+} influx, in latter study we only examined the cAMP effect on the first $[Ca^{2+}]_i$ transient.

Cyclic AMP stimulates a cation whole-cell current in TRPC6-expressing HEK293 cells

Note that $[Ca^{2+}]_i$ transient is not only affected by Ca^{2+} movement across the plasma membrane, but also affected by Ca^{2+} movement across the membrane of intracellular Ca^{2+} stores. Thus $[Ca^{2+}]_i$ transient could not faithfully reflect the Ca^{2+} influx. Next we used whole-cell patch clamp to examine the effect of cAMP on TRPC6 activity on the plasma membrane. Application of 500 μM 8-Br-cAMP caused a marked increase in whole-cell cation current density in both inward and outward directions in TRPC6-expressing cells but not in vector-transfected group (Fig. 2A, B and C). The time course of cAMP activation was recorded at ±80 mV, and the results showed that cAMP activation on TRPC6 followed a relative slow time course. It peaked at ~10 min after 8-Br-cAMP application (Fig. 2D). We reason that two factors might have contributed to the difference in time kinetics between cAMP-induced $[Ca^{2+}]_i$ transient (Fig. 1A) and the cation current (Fig. 2D): 1) opening of a small percentage of TRPC6 might be enough for global $[Ca^{2+}]_i$ rises; 2) the falling phase of $[Ca^{2+}]_i$ transient was not related to the inactivation of TRPC6. In this aspect, it has been well documented that the falling phase of $[Ca^{2+}]_i$ transient mainly reflects Ca^{2+} sequestration into intracellular stores as well as Ca^{2+} extrusion into the extracellular medium (30,31).

Participation of PI3K-PKB-MEK-ERK1/2 signaling pathway

One downstream target of cAMP is PI3K (17-20), the activity of which stimulates PKB-MEK-ERK1/2 pathway. In $[Ca^{2+}]_i$ measurement studies with TRPC6-expressing cells, two PI3K inhibitors wortmannin (100 nM) and LY294002 (30 μM) both markedly reduced the percentage of cells responding to 8-Br-cAMP (500 μM), Db-cAMP (300 μM), and forskolin (10 μM) (Fig. 3A and 3B, Fig. S1A and S1B). These two inhibitors also reduced the peak amplitude of the first $[Ca^{2+}]_i$ transient among the $[Ca^{2+}]_i$ responding cells (Fig. 3B, Fig. S1B). Three MEK inhibitors, including PD98059 (20 μM), U0126 (10 μM) and MEK inhibitor I (1 μM), had similar inhibitory effect on 8-Br-cAMP-, Db-cAMP-, and forskolin-induced Ca^{2+} influx in TRPC6-expressing cells (Fig. 3A and B, Fig. S1A and B).

Effect of PI3K inhibitors and MEK inhibitors on TRPC6-mediated cation currents was also examined. As shown in Fig. 3C, 8-Br-cAMP (500 μM)-stimulated whole-cell cation currents, which were recorded at ±80 mV, were significantly inhibited by PI3K inhibitors wortmannin (100 nM) and LY294002 (30 μM). MEK inhibitors PD98059 (20 μM), U0126 (10 μM), and MEK inhibitor I (1 μM) had similar inhibitory effect (Fig. 3C).

We tested whether 8-Br-cAMP could enhance MEK and ERK1/2 phosphorylation. Fig. 4 showed that 8-Br-cAMP (500 μM) induced a rapid MEK and ERK1/2 phosphorylation within 2 min and lasted for 10 min (Fig. 4A and B). The total MEK and ERK1/2 protein levels were not affected by 8-Br-cAMP. PI3K is an upstream signaling molecule of MEK and ERK1/2. As expected, in the presence of PI3K inhibitor LY294002 (30 μM), cAMP was unable to stimulate MEK and ERK1/2 phosphorylation (Fig. 4C and D). Likewise, inhibition of MEK (by U0126, 10 μM), which is an upstream signal molecule of ERK1/2, prevented the cAMP-induced phosphorylation of ERK1/2 (Fig. 4D).

Direct ERK1/2 phosphorylation on TRPC6

There are four ERK1/2 consensus sites (Pro-X-Ser or Thr-Pro) in TRPC6 proteins. Point mutation was made at each of these four sites. These constructs were transfected into HEK293 cells. One mutant $TRPC6^{S281G}$ abolished the cAMP activation on TRPC6 in whole-cell patch recording (Fig. 5A and B). Other mutants of TRPC6, including S194G, T220A and S768G, did not alter the cAMP response (data not shown). Cell-attached single-channel patch recorded a cAMP-activated channel in TRPC6-expressing cells (Fig. 5C) whereas cAMP failed to activate this channel in $TRPC6^{S281G}$-expressing cells (Fig. 5C and D). These results suggest that ERK1/2 may directly activate TRPC6 by phosphorylating at Ser-281.

Lack of involvement of PKA, PKG and EPAC

In $[Ca^{2+}]_i$ measurement experiments, a PKG inhibitor KT5823 (1 μM) and two PKA inhibitors KT5720 (1 μM) and H89 (10 μM) had no effect either on the percentage of cells responding to 8-Br-cAMP (Fig. S2A) or on the peak amplitude of the first $[Ca^{2+}]_i$ transient among the responding cells (Fig. S2B). We also utilized a TRPC6 mutant $TRPC6^{T69A+S321A}$, in which effective PKG phosphorylation sites were mutated (10). This mutant displayed the cAMP-induced $[Ca^{2+}]_i$ responses similar to that of wild-type TRPC6 (Fig. S2A and B). EPAC is another possible downstream target of cAMP. However, a selective EPAC agonist 8-pCPT-2'-O-Me-cAMP only had a very small stimulating action on $[Ca^{2+}]_i$ rise, suggesting that the involvement of EPAC, if any, was small (Fig. S2A and B).

Whole-cell patch clamp studies were used to verify the above findings. The results showed that KT5720 and KT5823 treatments had no effect on 8-Br-cAMP-stimulated whole-cell cation current in TRPC6-expressing cells (Fig. S2D). Furthermore, 8-pCPT-2'-O-Me-cAMP failed to stimulate the whole-cell cation current in TRPC6-expressing cells (Fig. S2C). Taken together, these data suggest that the stimulating action of cAMP on TRPC6 did not involve PKA, PKG, and EPAC.

Lack of cAMP effect on TRPC6 translocation

One report suggested that cAMP may be a key signal that facilitates TRPC6 trafficking to the plasma membrane (32). We used total internal fluorescence reflection microscopy (TIRFM), a powerful technique for studying protein movements within the periplasmic space, to monitor the movement of GFP-tagged TRPC6 towards the plasma membrane (33). GFP-tagged TRPC6 was transfected into HEK293 cells and the cells were treated with 8-Br-cAMP (500 μM) for 5-10 minutes. It was found that 8-Br-cAMP had no effect on TRPC6 fluorescence change in the plasma membrane region (Fig. S3A and D). Pmem-YFP, which is the fluorescent marker of the plasma membrane, was used as the time control. Pmem-YFP fluorescence did not change in 10 min (Fig. S3B and D). This control excluded the possibility of plasma membrane movement in the axial direction during the experiments. A positive control was also

included, in which TG (4 μM) was shown to stimulate the translocation of heteromeric TRPV4-C1 channels to the plasma membrane as reported elsewhere (Fig. S3C and D) (33). As another control, GFP-tagged TRPC6 could also be activated by 8-Br-cAMP in whole-cell recording (Fig. S4). Taken together, these data demonstrated that cAMP did not alter the translocation of TRPC6 to the plasma membrane.

cAMP-PI3K-PKB-MEK-ERK1/2-TRPC6 signaling cascade in glomerular messangial cells

Recent studies showed that glucagon binds specific receptors to increase cAMP production and to cause $[Ca^{2+}]_i$ rises in glomerular mesangial cells, and that the MEK and ERK1/2 pathway is involved in the processes (21,22). Furthermore, TRPC6 is known to be abundantly expressed in glomerular mesangial cells (3). Thus we explored the functional role of PI3K-PKB-MEK-ERK1/2-TRPC6 signaling cascade in glucagon-induced Ca^{2+} influx in renal glomerular mesangial cells. The results showed that glucagon (10 nM) and 8-Br-cAMP (500 μM) induced $[Ca^{2+}]_i$ rises in glomerular mesangial cells (Fig. 6A-B). The $[Ca^{2+}]_i$ rises were abolished by the omission of extracellular Ca^{2+}, but were not affected by thapsigargin pretreatment, suggesting an involvement of Ca^{2+} influx but not intracellular Ca^{2+} store release (Fig. 6A-D). The $[Ca^{2+}]_i$ rises were inhibited by LY294002 and U0126 treatments (Fig. 6C and D). In immunoblot studies, glucagon (10 nM) and 8-Br-cAMP (500 μM) were both able to induce phosphorylation of MEK and ERK1/2 in a time-dependent manner in mesangial cells (Fig. S5). To verifying the involvement of TRPC6, siRNA strategy was employed. In immunoblot, TRPC6-specific siRNA effectively reduced the expression level of TRPC6 proteins in mesangial cells (Fig. 6E). In functional studies, TRPC6-specific siRNA abolished the glucagon- and cAMP-induced $[Ca^{2+}]_i$ rises in these cells (Fig. 6F). These data suggested that glucagon-induced Ca^{2+} influx in glomerular mesangial cells was mediated through cAMP-PI3K-PKB-MEK-ERK1/2-TRPC6 pathway.

DISCUSSION

The major findings of this study are as follows: 1) Cyclic AMP and forskolin evoked Ca^{2+} influx and elicited a whole-cell cation current in TRPC6-expressing HEK293 cells. 2) The effect of cAMP on TRPC6 was inhibited by pharmacological antagonists of PI3K and MEK. Furthermore, cAMP could induce the phosphorylation of MEK and its downstream target ERK1/2. Importantly, point mutation at ERK1/2 phosphorylation sites on TRPC6 proteins ($TRPC6^{S281G}$) abolished the cAMP activation on TRPC6-mediated cation current in whole-cell and single-channel recordings. 3) Glucagon and cAMP could both induce $[Ca^{2+}]_i$ rises in the primary cultured rat glomerular mesangial cells, the effect of which was abolished by a TRPC6-specific siRNA and inhibitors of PI3K and MEK. These data provide strong evidence that cAMP acts through PI3K-PKB-MEK-ERK1/2 to activate TRPC6 in both TRPC6-expressing HEK293 cells and native glomerular mesangial cells (Schematic drawing in Fig. 7). It is likely that ERK1/2 directly phosphorylates Ser-281 of TRPC6 to activate the channels. These results added ERK1/2 to the list of protein kinases that can directly regulate TRPC6 via phosphorylation. This list includes Fyn, CAMKII, PKC and PKG (7,8), and now ERK1/2.

Two other reports have investigated the effect of cAMP and PKA on TRPC6 (11,32). One report shows that PKA had no effect on TRPC6 activity (11), which is in agreement with the present study. Another report suggests an involvement of cAMP in agonist-induced translocation of TRPC6 proteins onto plasma

membrane in vascular endothelial cells (32). This is in contrast to the results of the present study in which we showed that cAMP does not stimulate TRPC6 translocation to the plasma membrane by TIRFM. The reason for this discrepancy is not clear, but it could be due to difference in cell types and/or methods used for monitoring translocation. We used TIRFM whereas the others used conventional confocal imaging (32). It is relatively easier to quantify the protein trafficking by TIRFM than by conventional confocal imaging.

The findings that cAMP-PI3K-PKB-MEK-ERK1/2 signaling pathway activates TRPC6 may have important physiological or pathological implications. It is well documented that MEK-ERK1/2 pathway and TRPC6 each plays important roles in regulating cell proliferation and differentiation (34-36). However, relationship between MEK-ERK1/2 and TRPC6 has never been established. In kidney, it was reported that a major hormone glucagon, through a signaling cascade involving cAMP, ERK1/2 and $[Ca^{2+}]_i$ rises (21,22), can stimulate the growth and proliferation of glomerular mesangial cells, resulting in glomerular injury (22,24). But the role of TRPC6 in the process is unclear. In the present study, we confirmed that glucagon and cAMP could elicit $[Ca^{2+}]_i$ rises in the primary cultured glomerular mesangial cells via PI3K-MEK-ERK1/2 pathway. More importantly, we found that suppressing TRPC6 expression level using a TRPC6-specific siRNA abolished the $[Ca^{2+}]_i$ rises in response to glucagon and cAMP. Taken together, these data strongly suggest that the glucagon-induced $[Ca^{2+}]_i$ rises in glomerular mesangial cells were mediated by TRPC6 through cAMP-PI3K-MEK-ERK1/2 axis. This Ca^{2+} influx is expected to stimulate the growth and proliferation of renal mesangial cells.

We used two compounds LY294002 and wortmannin to demonstrate the role of PI3K pathway in the cAMP activation of TRPC6. It has been shown that LY294002, in addition to its action on PI3K, could directly inhibit the activity of Ca^{2+} channels $Ca_v1.2$ (37). It is unknown whether LY294002 could also have direct inhibitory effect on TRPC6. However, in the present study, another PIK3 inhibitor wortmannin and multiple MEK inhibitors also exerted similar effect on the cAMP activation of TRPC6. Furthermore, point mutation at the ERK site prevented the cAMP activation of TRPC6. Therefore, it is safe to conclude that the PI3K-PKB-MEK-ERK1/2 pathway is involved.

In conclusion, the current study identified the cAMP-PI3K-MEK-ERK1/2 axis as a novel signaling pathway for TRPC6 activation. ERK1/2 phosphorylates on Ser-281 to activate TRPC6. We also found that the cAMP-PI3K-PKB-MEK-ERK1/2-TRPC6 signaling pathway plays a key role in glucagon-induced Ca^{2+} influx in renal glomerular mesangial cells.

ACKNOWLEDGMENTS

This work was supported by Hong Kong RGC Grants (CUHK477408, CUHK479109 and CUHK478710), Focused Investment Scheme and Li Ka Shing Institute of Health Sciences.

ABBREVIATIONS

cAMP	Cyclic AMP
TRPC6	Canonical transient receptor potential 6 channels
TIRFM	Total internal fluorescence reflection microscopy
PI3K	Phosphatidylinositol 3-kinase
ERK1/2	Extracellular signals regulated kinase 1 and 2
MEK	Mitogen-activated protein kinase kinase
CNG	Cyclic nucleotide-gated
EPAC	Exchange protein activated by cAMP
PKA	Protein kinase A
PKC	Protein kinase C
PKG	Protein kinase G
PKB	Protein kinase B
DAG	Diacylglycerol
HEK	Human embryonic kidney
TG	Thapsigargin

REFERENCES

1. Dietrich, A., and Gudermann, T. (2007) *Handb Exp Pharmacol*, **179,** 125-141
2. Zhou, J., Du, W., Zhou, K., Tai, Y., Yao, H., Jia, Y., Ding, Y., and Wang, Y. (2008) *Nat Neurosci* **11**, 741-743
3. Graham, S., Ding, M., Sours-Brothers, S., Yorio, T., Ma, J. X., and Ma, R. (2007) *Am J Physiol Renal Physiol* **293**, F1381-1390
4. Winn, M. P., Conlon, P. J., Lynn, K. L., Farrington, M. K., Creazzo, T., Hawkins, A. F., Daskalakis, N., Kwan, S. Y., Ebersviller, S., Burchette, J. L., Pericak-Vance, M. A., Howell, D. N., Vance, J. M., and Rosenberg, P. B. (2005) *Science* **308**, 1801-1804
5. Nilius, B., and Owsianik, G. (2010) *Pflugers Arch* **460**, 437-450
6. Hofmann, T., Obukhov, A. G., Schaefer, M., Harteneck, C., Gudermann, T., and Schultz, G. (1999) *Nature* **397**, 259-263
7. Hisatsune, C., Kuroda, Y., Nakamura, K., Inoue, T., Nakamura, T., Michikawa, T., Mizutani, A., and Mikoshiba, K. (2004) *J Biol Chem* **279**, 18887-18894
8. Shi, J., Mori, E., Mori, Y., Mori, M., Li, J., Ito, Y., and Inoue, R. (2004) *J Physiol* **561**, 415-432
9. Kim, J. Y., and Saffen, D. (2005) *J Biol Chem* **280**, 32035-32047
10. Takahashi, S., Lin, H., Geshi, N., Mori, Y., Kawarabayashi, Y., Takami, N., Mori, M. X., Honda, A., and Inoue, R. (2008) *J Physiol* **586**, 4209-4223
11. Hassock, S. R., Zhu, M. X., Trost, C., Flockerzi, V., and Authi, K. S. (2002) *Blood* **100**, 2801-2811
12. Rall, T. W., and Sutherland, E. W. (1958) *J Biol Chem* **232**, 1065-1076
13. Defer, N., Best-Belpomme, M., and Hanoune, J. (2000) *Am J Physiol Renal Physiol* **279**, F400-416
14. Bos, J. L. (2006) *Trends Biochem Sci* **31**, 680-686
15. Schwede, F., Maronde, E., Genieser, H., and Jastorff, B. (2000) *Pharmacol Ther* **87**, 199-226
16. Pelligrino, D. A., and Wang, Q. (1998) *Prog Neurobiol* **56**, 1-18
17. Schulte, G., and Fredholm, B. B. (2003) *Exp Cell Res* **290**, 168-176
18. Schulte, G., and Fredholm, B. B. (2003) *Cell Signal* **15**, 813-827
19. Schulte, G., and Fredholm, B. B. (2000) *Mol Pharmacol* **58**, 477-482
20. Webster, C. R., and Anwer, M. S. (1999) *Am J Physiol* **277**, G1165-1172
21. Li, X. C., Carretero, O. A., and Zhuo, J. L. (2006) *Biochem Pharmacol* **71**, 1711-1719
22. Li, X. C., Carretero, O. A., Shao, Y., and Zhuo, J. L. (2006) *Hypertension* **47**, 580-585
23. Shah, P., Vella, A., Basu, A., Basu, R., Schwenk, W. F., and Rizza, R. A. (2000) *J Clin Endocrinol Metab* **85**, 4053-4059
24. Hostetter, T. H. (2003) *Semin Nephrol* **23**, 194-199
25. Zhang, X., Chen, X., Wu, D., Liu, W., Wang, J., Feng, Z., Cai, G., Fu, B., Hong, Q., and Du, J. (2006) *J Am Soc Nephrol* **17**, 1532-1542
26. Ferdows, M., Golchini, K., Adler, S. G., and Kurtz, I. (1989) *Kidney Int* **35**, 783-789
27. Soboloff, J., Spassova, M., Xu, W., He, L. P., Cuesta, N., and Gill, D. L. (2005) *J Biol Chem* **280**, 39786-39794
28. De Young, G. W., and Keizer, J. (1992) *Proc Natl Acad Sci U S A* **89**, 9895-9899
29. Li, Y. X., Rinzel, J., Keizer, J., and Stojilkovic, S. S. (1994) *Proc Natl Acad Sci U S A* **91**,

58-62
30. Wang, X., Reznick, S., Li, P., Liang, W., and van Breemen, C. (2002) *Cell Calcium* **31**, 265-277
31. Mountian, I., Manolopoulos, V. G., De Smedt, H., Parys, J. B., Missiaen, L., and Wuytack, F. (1999) *Cell Calcium* **25**, 371-380
32. Fleming, I., Rueben, A., Popp, R., Fisslthaler, B., Schrodt, S., Sander, A., Haendeler, J., Falck, J. R., Morisseau, C., Hammock, B. D., and Busse, R. (2007) *Arterioscler Thromb Vasc Biol* **27**, 2612-2618
33. Ma, X., Cao, J., Luo, J., Nilius, B., Huang, Y., Ambudkar, I. S., and Yao, X. (2010) *Arterioscler Thromb Vasc Biol*. **30,** 2249-2455.
34. Roberts, P. J., and Der, C. J. (2007) *Oncogene* **26**, 3291-3310
35. El Boustany, C., Bidaux, G., Enfissi, A., Delcourt, P., Prevarskaya, N., and Capiod, T. (2008) *Hepatology* **47**, 2068-2077
36. Ding, X., He, Z., Shi, Y., Wang, Q., and Wang, Y. (2010) *Expert Opin Ther Targets* **14**, 513-527
37. Welling, A., Hofmann, F., Wegener, J. W. (2005) *Mol Pharmacol* **67**, 541-544.

FIGURE LEGENDS

Fig. 1 8-Br-cAMP-induced $[Ca^{2+}]_i$ rises in HEK293 cells. (A and B) Representative traces showing 500 μM 8-Br-cAMP-induced $[Ca^{2+}]_i$ rises in the absence (A) and presence (B) of 4 μM thapsigargin (TG) in TRPC6-expressing HEK293 cells. (C and D) Summary of data showing the percentage of $[Ca^{2+}]_i$ responding cells (C) and the peak amplitude of the first $[Ca^{2+}]_i$ transient among the responding cells (D) to 500 μM 8-Br-cAMP. T6, TRPC6-expressing; Vec, vector-transfected control; WT, wild-type HEK293 cells. Mean ± SEM (n = 5–12 independent experiments, 15 to 40 cells per experiment). $^*P< 0.05$ as compared to T6.

Fig. 2 8-Br-cAMP-stimulated whole-cell cation current density in HEK293 cells. (A) Representative traces showing voltage protocol (upper) and the corresponding whole-cell cation current before (middle) and after (lower) 500 μM 8-Br-cAMP application in TRPC6-expressing cells. (B and C) Current–voltage relationships before and after 500 μM 8-Br-cAMP treatment in vector-transfected (B) and TRPC6-expressing (C) cells. (D) Representative time course of 8-Br-cAMP (500 μM)-stimulated whole-cell cation current density at ±80 mV in TRPC6-expressing cells. Mean ± SEM (n = 5–6 cells).

Fig. 3 Effects of PI3K and MEK inhibitors on 8-Br-cAMP-induced $[Ca^{2+}]_i$ rises and whole-cell cation current in TRPC6-expressing HEK293 cells. (A and B), $[Ca^{2+}]_i$ rises; (C), whole-cell cation current. Shown were data summary for the percentage of $[Ca^{2+}]_i$ responding cells (A), the peak amplitude of the first $[Ca^{2+}]_i$ transient among the responding cells (B), and the maximal whole-cell cation current density at ±80 mV (C) in response to 8-Br-cAMP under different treatments. The cAMP-activated currents were obtained by subtracting currents before cAMP treatment from those after cAMP treatment. 8-Br-cAMP, 500 μM; wortmannin (Wort, 100 nM); LY294002, (LY, 30 μM); MEK inhibitor I (MEK, 1 μM); PD98059 (PD, 20 μM), U0126 (U0126, 10 μM). Mean ± SEM (for Ca^{2+} measurements, n = 4–8 independent experiments, 15 to 40 cells per experiment; for whole-cell recording, n = 4–5 cells). $^*P< 0.05$ as compared to control.

Fig. 4 Time-dependent changes of phosphorylated and total MEK and ERK1/2 in TRPC6-expressing HEK293 cells. Shown were representative images (top) and summary (bottom) of immunoblot experiments showing time-dependent responses of MEK (A and C) and ERK1/2 (B and D) to 500 μM 8-Br-cAMP. (C and D) In the presence of 30 μM LY294002 or 10 μM U0126. p-MEK, phosphorylated MEK; MEK, total MEK; p-ERK1/2, phosphorylated ERK1/2; ERK1/2, total ERK1/2. Mean ± SEM (n = 3–5 independent experiments). $^*P< 0.05$ as compared to 0 min.

Fig. 5 Effect of point mutation at Ser-281 on 8-Br-cAMP-stimulated cation current in TRPC6-expressing HEK293 cells. (A and B) Whole-cell current–voltage relationships before and after 500 μM 8-Br-cAMP application in cells transfected with wild-type TRPC6 (A) and $TRPC6^{S281G}$ (B). (C) Representative single channel traces in cell-attached patches before and after 500 μM 8-Br-cAMP application. Upper two traces, wild-type TRPC6-transfected cells; Bottom two traces, $TRPC6^{S281G}$-transfected cells. The pipette holding potential was at +60 mV. (D) Summary of data showing single-channel open probability (NPo) of TRPC6 channels before and after 8-Br-cAMP application. Mean ± SEM (n = 4-10 cells/patches) $^*P< 0.05$ as compared to wild-type TRPC6 after 8-Br-cAMP application.

Fig. 6 8-Br-cAMP- and glucagon-induced $[Ca^{2+}]_i$ rises in the primary cultured rat glomerular mesangial cells. (A and B) Representative traces showing 500 μM 8-Br-cAMP- (A) and 20 nM glucagon- (B) induced $[Ca^{2+}]_i$ rises in the absence (gray line) and presence (black line) of 1 mM extracellular Ca^{2+}. (C and D) Summary of data showing the peak magnitude of $[Ca^{2+}]_i$ rises to 500 μM 8-Br-cAMP (C) and 10 nM glucagon (D) under different conditions. Control, NPSS; TG-treated, after thapsigargin treatment; LY, LY294002 (30 μM); U0126, U0126 (10 μM). (E) Representative images (top) and summary of data (bottom) showing the effect of TRPC6-siRNA on TRPC6 protein expression in glomerular mesangial cells. Control was transfected with scrambled siRNA. (F) Summary of data showing the effect of TRPC6-siRNA on 8-Br-cAMP- and glucagon-induced $[Ca^{2+}]_i$ rises. Mean ± SEM (n = 3–9 independent experiments and 15 to 40 cells per experiment in Ca^{2+} measurement, n = 3 experiments in immunoblots). $^{*}P < 0.05$ as compared to respective controls.

Fig. 7 Schematic figure showing the signal transduction pathway involving cAMP-PI3K-PKB-MEK-ERK1/2-TRPC6.

Figure 1

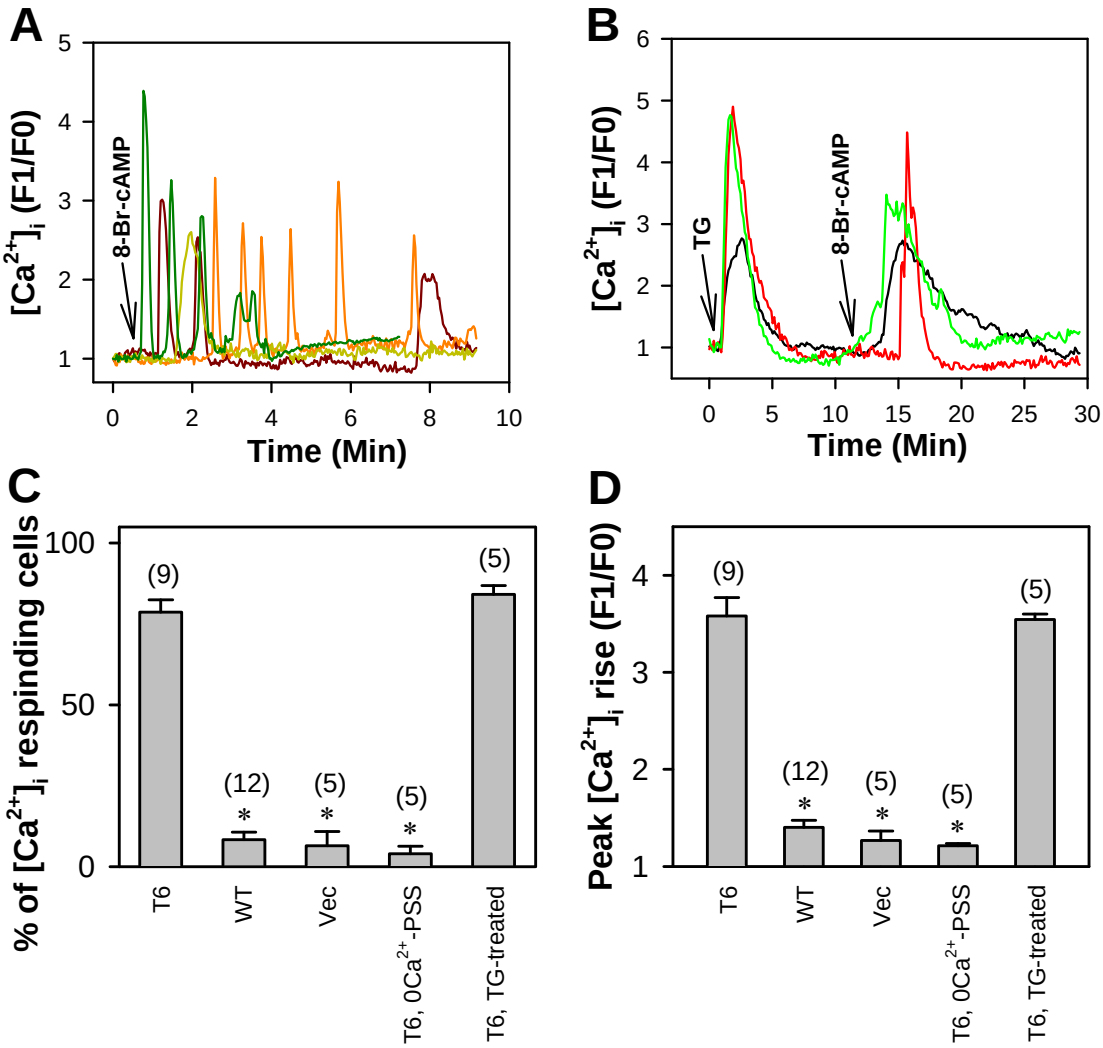

Figure 2

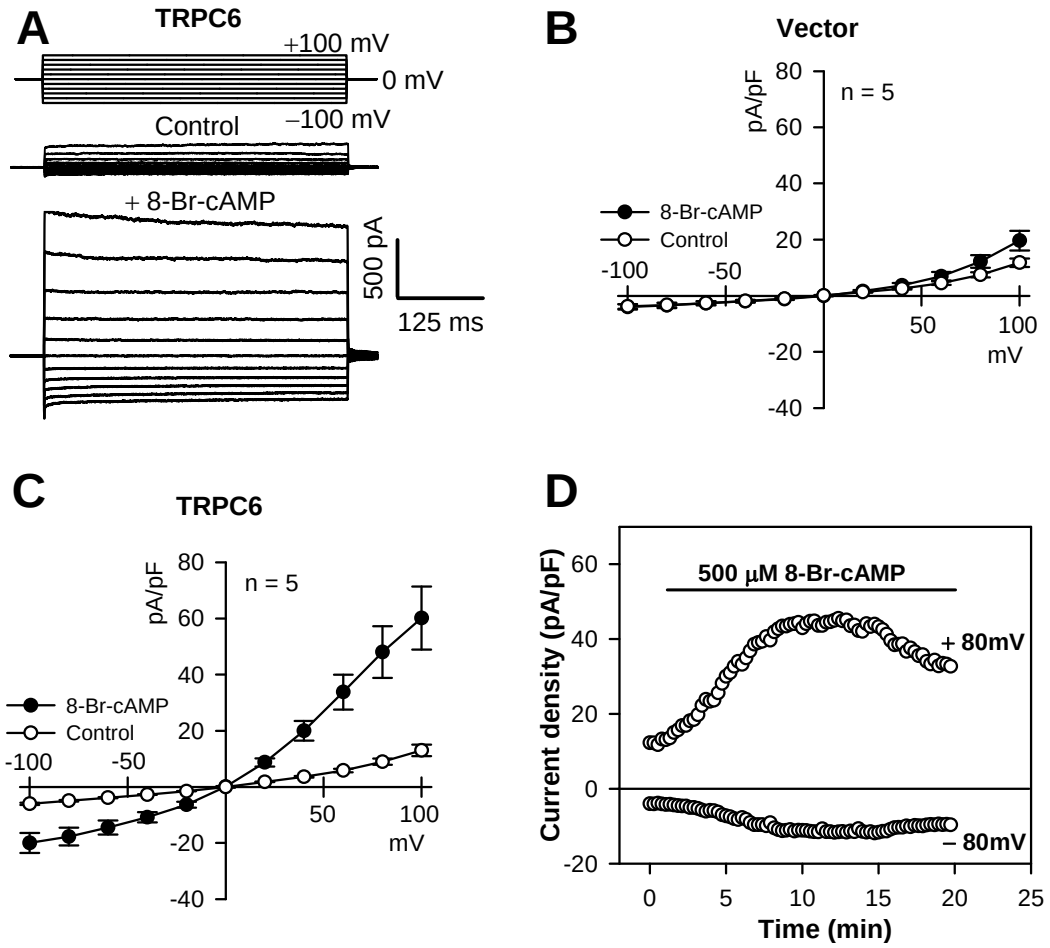

Figure 3

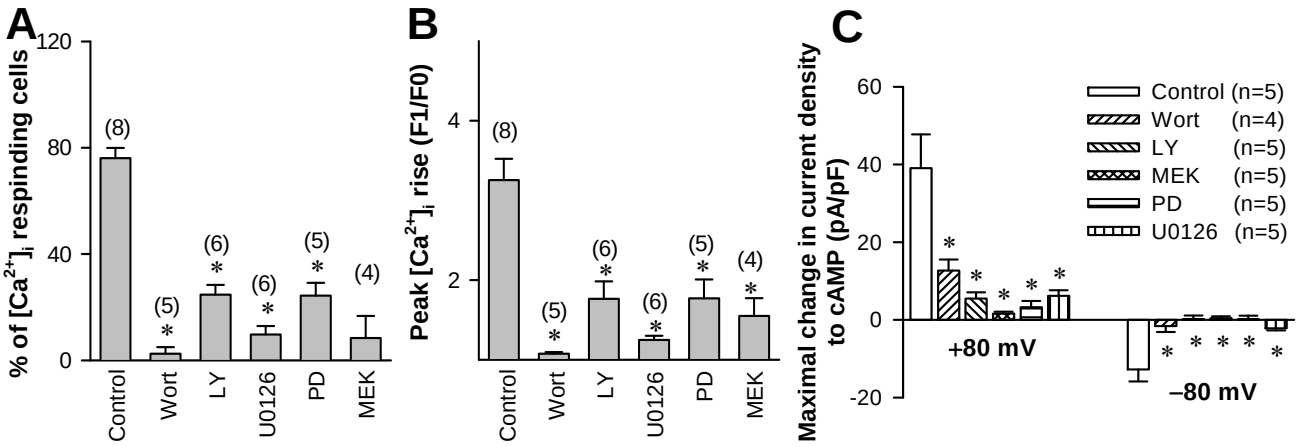

Figure 4

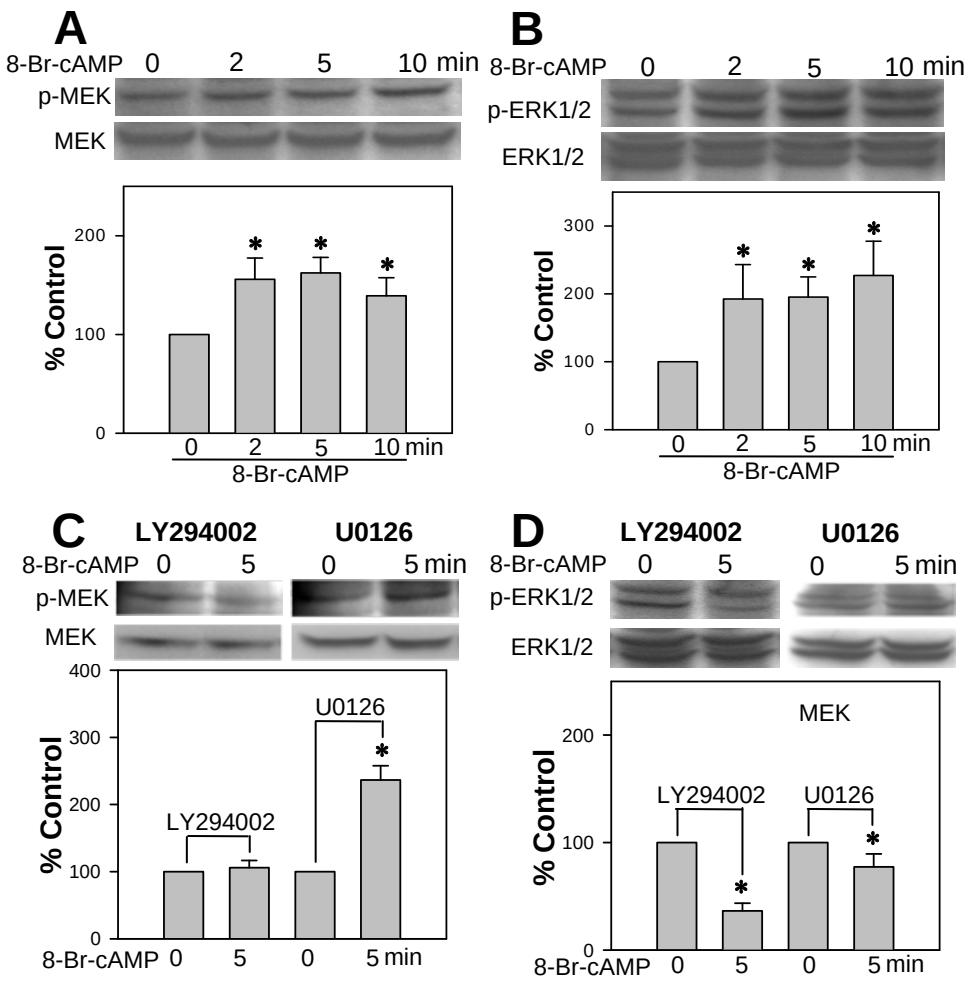

Figure 5

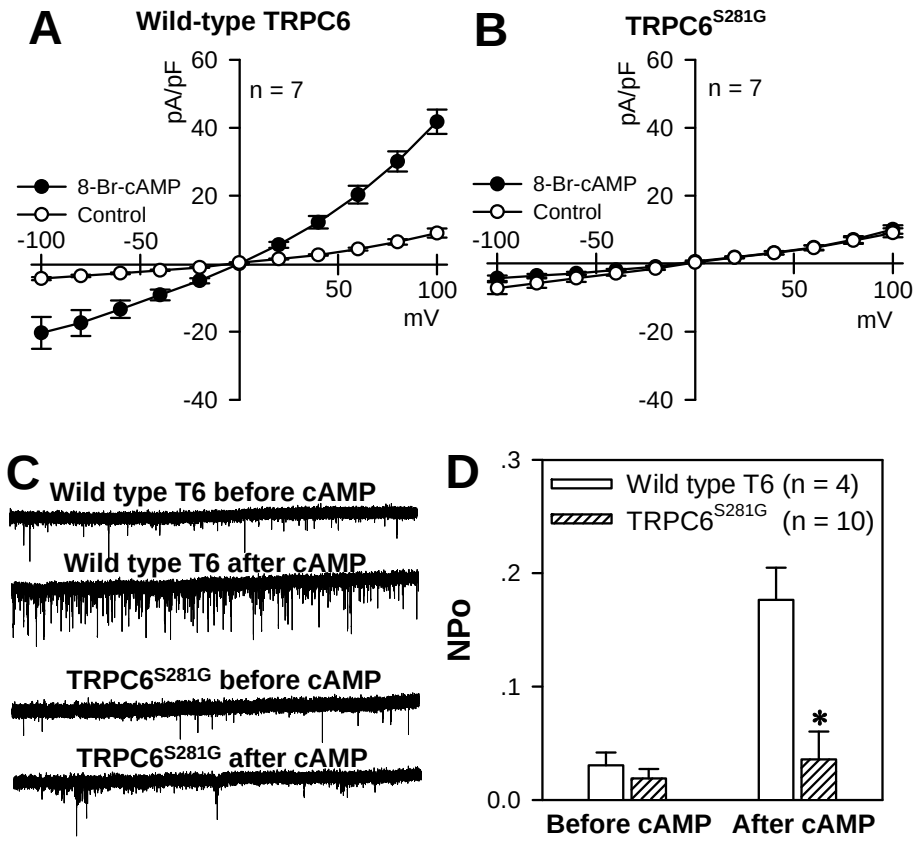

Figure 6

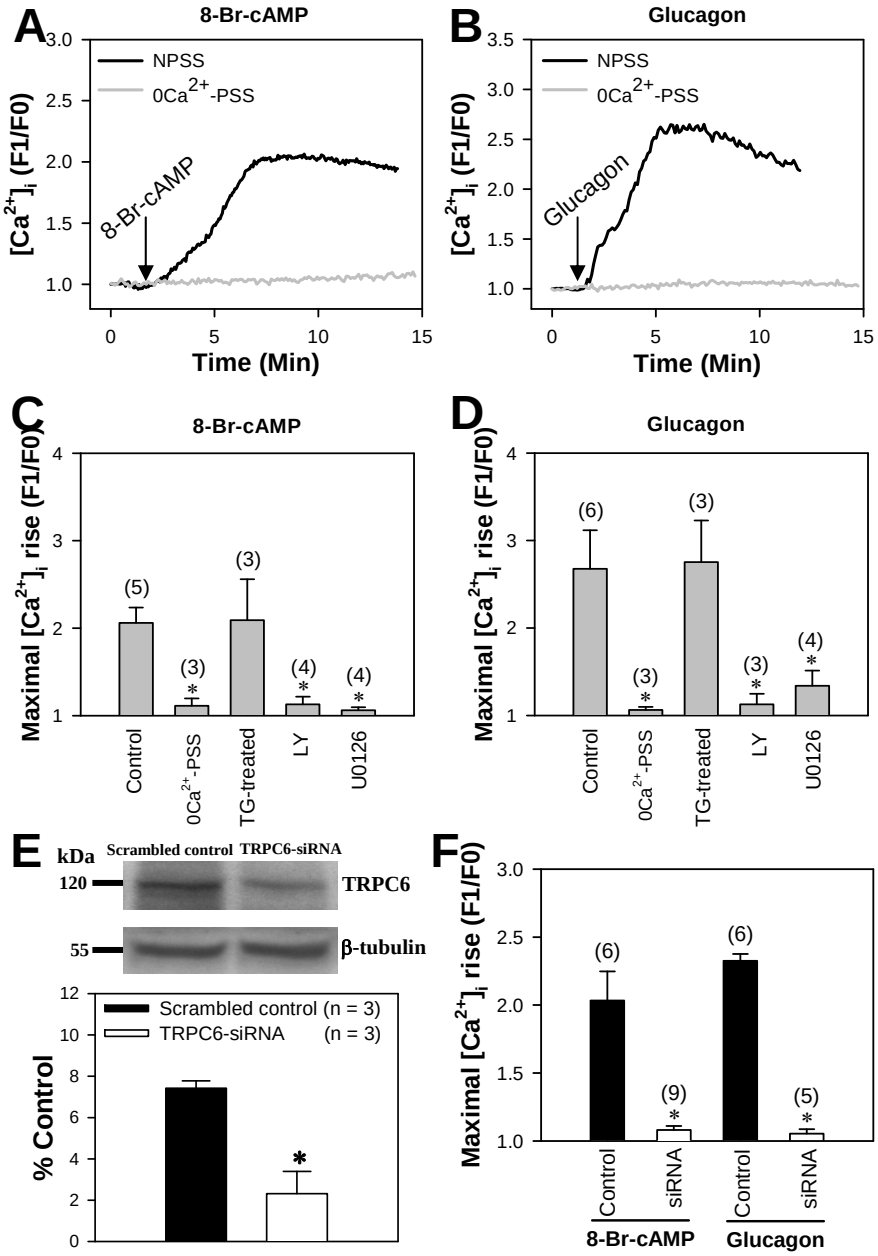

Figure 7